Synthesis and Characterization of Co/CdSe Core/Shell Nanocomposites: Bifunctional Magnetic-Optical Nanocrystals

Hyungrak Kim, Marc Achermann, Laurent P. Balet, Jennifer A. Hollingsworth, and Victor I. Klimov*

Chemistry Division, C-PCS, Los Alamos National Laboratory, Los Alamos, New Mexico 87545

Received May 17, 2004; E-mail: klimov@lanl.gov

Nano*composite* materials[1] provide the possibility for enhanced functionality and multifunctional properties in contrast with their more-limited *single-component* counterparts. One example of a nanocomposite material is the inorganic core−shell structure. In the case where semiconductors comprise the core and shell, the core−shell motif has permitted enhanced photoluminescence,[2] improved stability against photochemical oxidation,[2b,c,3] enhanced processability,[4] and engineered band structures.[5] Where metals have been combined in core−shell structures, noble metals have been grown on magnetic metal cores[6] and the reverse,[7] for example, causing changes in magnetic, optical, and chemical properties compared to those of the individual components.[6,7] While examples of enhancement or modification of properties resulting from the core−shell structures are becoming more common, instances of truly multifunctional behavior remain rare. For example, iron oxide nanoparticles overcoated with a dye-impregnated silica shell were shown to retain the magnetic properties of the core, while exhibiting the luminescent optical properties of the organic dye.[8] Here, we report a new type of nanocomposite, composed of a magnetic metal core, Co, and a semiconductor shell, CdSe. This provides a clear example of an *all-inorganic* bifunctional nanoparticle and is the first core/shell combination of a magnetic nanoparticle and a luminescent semiconductor quantum dot.

Co/CdSe core/shell nanocomposites were prepared by controlled CdSe deposition onto preformed Co nanocrystals (NCs). The Co NCs were synthesized by high-temperature decomposition of organometallic precursors, $Co_2(CO)_8$, in the presence of organic surfactant molecules.[9] After the reaction, the Co NCs were precipitated by the addition of a nonsolvent, anhydrous methanol, and redissolved in a nonpolar solvent such as toluene or hexane. By repeating this process, the Co NCs were effectively "washed" and excess surfactant was removed. For the core/shell preparation, washed Co NCs (2.7 mmol) were dispersed in *n*-hexane (∼2 mL). Trioctylphosphine oxide (TOPO, 99%; 10 g) and hexadecylamine (HDA, 99%; 5 g) were then heated to 120 °C under vacuum in a reaction flask. After 2 h, the TOPO and HDA were placed under nitrogen and heated to 140 °C. A small portion of this mixture (∼1 mL) was added to the Co NCs, and additional hexane was added if the resulting solution was very thick. This solution was then transferred back into the reaction flask. CdSe precursors (dimethylcadmium, 1.35 mmol, and Se, 1.5 mmol dissolved in 1.5 mL trioctylphosphine, in 5 mL additional TOP) were added dropwise into the vigorously stirred mixture. The reaction was held at temperature overnight. The low reaction temperature (in comparison with a conventional CdSe synthesis[10]) required a long incubation time. Further, higher temperatures (>200 °C) resulted in exclusively homogeneous nucleation and growth of CdSe NCs, unassociated with the Co NCs. While the lower-temperature preparation did generate some fraction

of both uncoated Co cores and unassociated CdSe NCs, the various fractions were isolable using a combination of standard size-selective precipitation/washing steps followed by magnetic separations. In general, methanol was used to destabilize the solutions, resulting first in precipitation of Co cores (brown solid) that could be redissolved in dichlorobenzene. CdSe NCs and Co/CdSe core/shell NCs were both soluble in hexane but could be separated by size. Further, by placing a magnet near a methanol-destabilized suspension, the core/shell NC component attracted to the magnet (note: the magnet had no impact on well-solubilized magnetic NCs). The emission from the composite particles was easily seen when excited by a hand-held fluorescent lamp.

The core Co NCs are reasonably monodisperse (±15−20%), with a diameter of ∼11 nm. The Co/CdSe core/shell NCs retain the spherical shape of the seed core and exhibit a uniform shell that is 2- to 3-nm thick (Figure 1a,b). The contrast between the Co core and CdSe shell is easily distinguishable by conventional TEM microscopy (Figure 1a), with the precise nanostructure of the shell visible in high-resolution (HR) imaging. As a possible mechanism for shell growth, we suggest a random, highly nonepitaxial, nucleation of CdSe on the Co surface followed by CdSe particle growth and nanocrystallite merging. The low growth temperature used for the CdSe deposition likely supports primarily heterogeneous rather than homogeneous nucleation, and the uniformity of the shell suggests a sufficient annealing process to build a complete coating.

As determined by powder X-ray diffraction (XRD) (Figure 2), the Co NCs grow as the ϵ-Co phase, which is typical of the preparative method employed here.[9] The Co/CdSe core/shell NCs yield an XRD pattern that contains additional diffraction peaks that can be indexed to wurtzite CdSe (confirmed in HR-TEM: ∼2.2 Å and ∼2.6 Å lattice spacings match the (110) and (102) crystal planes of wurtzite CdSe). The added broadness of the XRD reflections in the composite-structure pattern results from the very small domain size characteristic of the polycrystalline CdSe shell.[11]

DC magnetization as a function of temperature in an applied magnetic field of 100 Oe was recorded for the Co and the Co/CdSe NCs (Figure 3a). For 11 nm ϵ-Co NCs, the blocking temperature, T_B, is above 350 K, but the transition from superparamagnetic to ferromagnetic behavior after CdSe shell coating occurs at approximately 240 K (Figure 3a). Since no significant change in Co core size and shape was observed in TEM, the decrease in blocking temperature may be attributed largely to a decrease in interparticle magnetostatic interactions resulting from the change in encapsulation matrix from strictly organic surfactants to an inorganic CdSe layer.[12] No such modification of blocking temperature was observed when magnetic-optical nanocrystals were prepared as dimers.[13] The coercivity, the strength of a demagnetizing
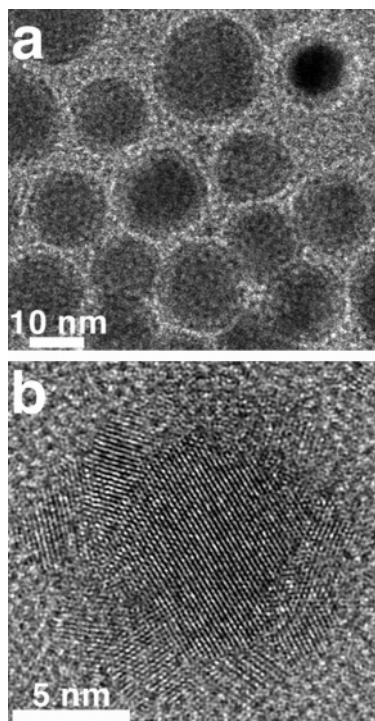
Figure 1. (a) TEM image of Co/CdSe core/shell nanocomposites. (b) High-resolution TEM image of a composite nanocrystal revealing the polycrystalline nature of the shell.
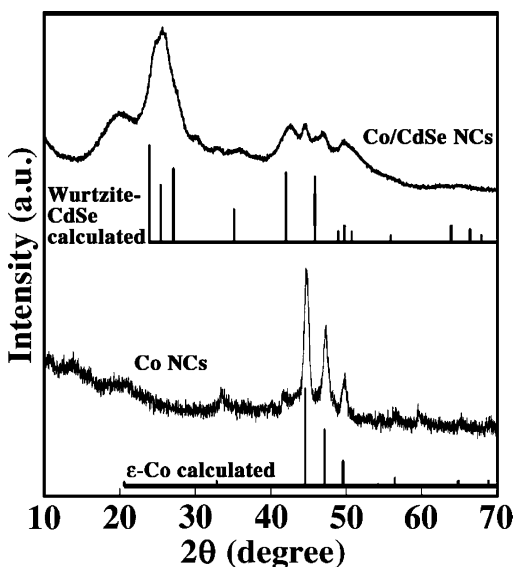
Figure 2. XRD patterns for Co NCs and Co/CdSe core/shell NCs compared to calculated patterns for ϵ-Co and wurtzite CdSe.

Figure 3. (a) Temperature dependence of the magnetization for field cooled (open) and zero field cooled (filled) Co NCs and Co/CdSe NCs; traces intersect at the blocking temperature, the transition from superparamagnetic to ferromagnetic behavior. (b) Field dependence of the magnetization for the same samples.
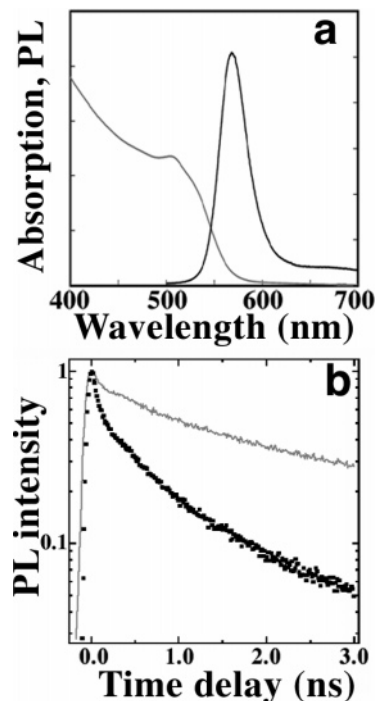
Figure 4. (a) UV absorption and photoluminescence spectra of Co/CdSe core/shell nanocomposites. (b) Normalized PL dynamics taken at 20 K of CdSe NCs (gray line) and Co/CdSe NCs (dotted line).

field required to coerce a magnetic particle to change magnetization direction, H_C, was also determined and found to be nearly the same for both samples, 0.11 T (Figure 3b), although there is a large drop in saturation magnetization per gram in the core/shell structures due to the presence of the nonmagnetic CdSe phase. The coercivity of single-domain NCs depends mainly on the magnetocrystalline anisotropy and the domain size of the particles. The consistency in coercivity between the two samples correlates well with TEM observations that magnetic-core particle size did not change appreciably. Further, it indicates that the coercivity is determined mainly by magnetocrystalline anisotropy, rather than surface anisotropy, which would be sensitive to surface modification.[11,13]

Absorption and emission spectra of the core/shell nanocomposites are presented in Figure 4a. The observation of a relatively large Stokes shift further distinguishes the core−shell NCs from pure CdSe quantum dots. Monodisperse CdSe nanoparticle solutions of
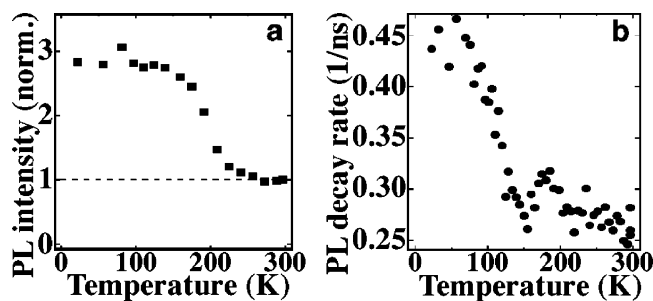
Figure 5. (a) PL$_{int}$ as a function of temperature, normalized at 300 K. (b) Temperature dependence of the decay rate of Co/CdSe NC emission.

similarly sized NQDs exhibit a Stokes shift of about 20 nm, compared to the nanocomposites' 40−50-nm shift. While the large Stokes shift may be related to the effect of the presence of a close-proximity nanomagnet on the semiconductor optical properties, it can also be attributed to CdSe shape anisotropy. Specifically, the crystallite domains visible in high-resolution TEM (Figure 1b) are approximately 2 × 3 nm in size. The absorption edge roughly correlates with a CdSe NC having these dimensions, but the photoluminescence (PL) maximum is shifted. Likely, pairs of neighboring domains are sufficiently well associated such that they behave as single "nanorods" causing the observed Stokes shift, similar to CdSe nanorod samples, where the Stokes shift is large compared to approximately spherical particles.[14] For the Co/CdSe NCs, we obtain a quantum yield (QY) in emission of ∼2−3%. While not optimized, this is comparable to QYs (5−6%) obtained for CdSe prepared by similar preparative routes without, for example, ZnS overcoating to enhance emission efficiency. In addition, we find that the PL dynamics of the Co/CdSe NCs is distinctly different from that for CdSe NCs (Figure 4b). At low temperatures (20 K), where trapping of excited carriers is strongly reduced and therefore PL dynamics of "plain" CdSe NCs is normally dominated by relatively slow radiative decay (time constant >50 ns),[15] we observe that the PL of the core/shell NCs decays very rapidly (within a few nanoseconds). Such accelerated PL decay can be due to increased rates of either radiative recombination (induced by magnetic interactions between the semiconductor and the metal components) or nonradiative decay (via, for example, quenching in the presence of the metallic core) or both. To clarify the mechanisms for the accelerated decay, we analyze the temperature dependence of the time-integrated emission intensity (PL$_{int}$) and the relaxation rate defined as the inverse of the decay time constant. The growth of PL$_{int}$ with decreasing temperature (Figure 5a) indicates the decrease of the ratio, η, of the nonradiative, R_{nr}, to radiative, R_r, decay rates. This decrease is accompanied by the growth of the total PL decay rate, $R = R_r + R_{nr}$ (Figure 5b), indicating that its radiative component, $R_r = R(1 + \eta)$, *increases* with decreasing temperature. Such behavior is highly unusual for nanoscale CdSe structures, for which the radiative recombination rate typically decreases as the temperature is decreased.[15] This finding indicates that the presence of the magnetic core significantly affects the effective strength of the "emitting" optical transition of the semiconductor shell, likely through modifying the spin structure of the lowest excitonic state.[16] Relatively low PL quantum yields of our samples indicate that the emission quenching by the metal core can also contribute to the acceleration of the PL dynamics. However, since the latter mechanism is not strongly temperature dependent, the observed increase of the total rate at low temperatures results primarily from the enhanced radiative decay.

In summary, a novel synthetic method was developed for the preparation of truly bifunctional, all inorganic NCs that combine the properties of magnetic nanoparticles and semiconductor quantum dots for the first time in a core/shell arrangement. While the nanocomposites retain the optical and magnetic properties of the component parts, permitting potential applications that would make use of this novel bifunctionality, e.g., optical "reporters" coupled with magnetic "handles" for use in bioassays, the respective properties are altered because of the unique core/shell structure. Studies are underway to improve QYs by overcoating the core/shell particles with a second, wider band-gap shell, such as ZnS, and, alternatively, to grow a spacer layer between the magnetic core and the semiconductor in order to minimize potential quenching of the shell by the metal core. Finally, spectroscopic investigations of the effect of magnetic interactions on semiconductor carrier recombination rates are also under further investigation.

References

(1) (a) Ajayan, P. M.; Schadler, L. S.; Braun, P. V. *Nanocomposites Science and Technology*; Wiley & Sons: New York, 2003. (b) Godovsky, D. Y. *Adv. Polym. Sci.* **2000**, *153*, 163−205. (c) Schmidt, H. K.; Geiter, E.; Menning, M.; Krug, H.; Becker, C.; Winkler, R. P. *J. Sol.-Gel Sci. Technol.* **1998**, *13*, 397−404. (d) Caruso, F. *Adv. Mater.* **2001**, *13*, 11−22. (e) Hanif, K. M.; Meulenberg, R. W.; Strouse, G. F. *J. Am. Chem. Soc.* **2002**, *124*, 11495−11502.
(2) (a) Hines, M. A.; Guyot-Sionnest, P. *J. Phys. Chem.* **1996**, *100*, 468. (b) Dabbousi, B. O.; Rodriguez-Viejo, J.; Mikulec, F. V.; Heine, J. R.; Mattoussi, H.; Ober, R.; Jensen, K. F.; Bawendi, M. G. *J. Phys. Chem. B* **1997**, *101*, 9463. (c) Peng, X. G.; Schlamp, M. C.; Kadavanich, A. V.; Alivisatos, A. P. *J. Am. Chem. Soc.* **1997**, *119*, 7019−7029. (d) Micic, O. I.; Smith, B. B.; Nozik, A. J. *J. Phys. Chem. B* **2000**, *104*, 12149. (e) Cao, Y. W.; Banin, U. *Angew. Chem., Int. Ed.* **1999**, *38*, 3692.
(3) Correa-Duarte, M. A.; Giersig, M.; Liz-Marzán, L. M. *Chem. Phys. Lett.* **1998**, *286*, 497−501.
(4) Danek, M.; Jensen, K. F.; Murray, C. B.; Bawendi, M. G. *Chem. Mater.* **1996**, *8*, 173−180.
(5) (a) Kim, S.; Fisher, B.; Eisler, H.-J.; Bawendi, M. *J. Am. Chem. Soc.* **2003**, *125*, 11466−11467. (b) Eychmueller, A.; Vobmeyer, T.; Mews, A.; Weller, H. *J. Lumin.* **1994**, *58*, 223−226.
(6) Carpenter, E. E.; Sangregorio, C.; O'Connor, C. J. *IEEE Trans. Magn.* **1999**, *35*, 3496−3498.
(7) (a) Sobal, N. S.; Ebels, U.; Möhwald, H.; Giersig, M. *J. Phys. Chem. B* **2003**, *107*, 7351−7354. (b) Sobal, N. S.; Hilgendorff, M.; Mohwald, H.; Giersig, M.; Spasova, M.; Radetic, T.; Farle, M. *Nano Lett.* **2002**, *2*, 621−624.
(8) Lu, Y.; Yin, Y.; Mayers, B. T.; Xia, Y. *Nano Lett.* **2002**, *2*, 183−186.
(9) Dinega, D. P.; Bawendi, M. G. *Angew. Chem., Int. Ed.* **1999**, *38*, 1788−1791.
(10) Murray, C. B.; Norris, D. J.; Bawendi, M. G. *J. Am. Chem. Soc.* **1993**, *115*, 8706−8715.
(11) (a) Vestal, C. R.; Zhang, Z. J. *Nano Lett.* **2003**, *3*, 1739−1743, (b) Vestal, C. R.; Zhang, Z. J. *J. Am. Chem. Soc.* **2002**, *124*, 14312−14313.
(12) Gu, H. W.; Zheng, R. K.; Zhang, X. X.; Xu, B. *J. Am. Chem. Soc.* **2004**, *126*, 5664−5665.
(13) (a) Labaye, Y.; Crisan, O.; Berger, L.; Greneche, J. M.; Coey, J. M. D. *J. Appl. Phys.* **2002**, *91*, 8715−8717. (b) Papaefthymiou, G. C. *Mater. Res. Soc. Symp. Proc.* **2001**, *635*, C241−C247.
(14) Wang, X.-Y.; Zhang, J.-Y.; Nazzal, A.; Darragh, M.; Xiao, M. *Appl. Phys. Lett.* **2002**, *81*, 4829−4831.
(15) Crooker, S. A.; Barrick, T.; Hollingsworth, J. A.; Klimov, V. I. *Appl. Phys. Lett.* **2003**, *82*, 2793−2795.
(16) Efros, A. L.; Rosen, M.; Kuno, M.; Nirmal, M.; Norris, D. J.; Bawendi, M. *Phys. Rev. B* **1996**, *54*, 4843−4856.

JA047107X